J Mater Sci (2007) 42:9145–9153
DOI 10.1007/s10853-007-1933-y

From Ti–Al- to Ti–Al–N-sputtered 2D materials

Maria Teresa Vieira · Ana S. Ramos · José M. Castanho · João C. Oliveira · Albano Cavaleiro

Received: 30 November 2006 / Accepted: 11 June 2007 / Published online: 28 July 2007

Abstract This paper reviews thin films constituted by elements based on the Ti–Al–N system, bearing in mind the role of the condensed phases in the development of structural components and functional devices. In recent decades, the Ti–Al, Ti–N and Al–N nanocrystalline binary systems have rapidly attracted research and industry interest. These systems have revealed a great performance via atomic-level structural control, making it possible to tailor new atomic structures and morphologies suitable in different applications as protective and hard coatings and as thermal/diffusion barriers. The binary phases based on nitrogen were the first to exhibit a wealth of interesting mechanical and electrochemical behaviours. However, more recently the Ti-Al and, particularly, the $Ti_{1-x}Al_xN$ thin films have been applied with success in the industry. The purpose of this paper is to compile the master results concerning the production and characterisation of binary and ternary thin films of the Ti–Al–N system using similar deposition strategies. These materials form a good base to analyse the correlation between the chemical composition and the atomic structure, the preferred orientations and the morphology of 2D monolithic materials. The deposition strategies adopted and the thin films' chemical compositions determine the as-deposited structures and, consequently, the mechanical behaviour of the thin films produced, particularly the hardness. In general, an intermediary amorphous stage is observed, i.e., the thin films exhibit a loss of crystallinity in the transition from a saturated solid solution to a new compound.

M. T. Vieira (✉) · A. S. Ramos · J. M. Castanho · J. C. Oliveira · A. Cavaleiro
ICEMS, Departamento de Engenharia Mecânica, Faculdade de Ciências e Tecnologia, Universidade de Coimbra, R. Luís Reis Santos, Coimbra 3030-788, Portugal
e-mail: teresa.vieira@dem.uc.pt

Introduction

The Ti–Al–N equilibrium diagram contains phases that singly or mixed have had great technological impact, particularly as thin films, with the exception of Ti–Al which is famous for the bulk γ-based titanium aluminide. However, as a thin film γ-TiAl has recently shown a particularly strong potential for high temperature structural, electronic and biomedical applications [1–3], due to its high melting point, high specific strength, high elastic modulus, light weight and good oxidation resistance up to 800 °C [4]. During the last decade, the authors have been using thin films of the Ti–Al system as predictive alloys for bulk materials by extrapolating the properties of 2D (thin films) to 3D materials [5, 6]. TiAl thin films can also be deposited as an interlayer to promote better adhesion between thin films and substrates. This procedure has been successfully used with different nitrides [7] and particularly in TiAlN thin films for cutting tools [8]. Moreover, Ti–Al thin films, which can also be used to join materials, holds special interest for (micro)manufacturing [9].

The other binary systems with great impact are the Ti–N and the Al–N. TiN is the thin film most studied for diffusion barriers in microelectronics and in structural applications, such as the coating of cutting tools and mechanical components submitted during their life to wear and corrosive environments. This nitride exhibits a wide range of properties as a function of the N/Ti ratio, being the lowest

hardness values associated with the highest ratios (N/Ti ≥ 1.1) [10]. For substoichiometric thin films a hardness of 40 GPa can be attained, but close to stoichiometry the hardness values range from 20 to 30 GPa [10]. Although less studied than TiN, there are quite a number of publications on the deposition of AlN thin films by sputtering. Most of the published work concerns the application of AlN in the electronic and optoelectronic industries [11]. AlN is a very interesting material owing to its chemical stability and its high oxidation resistance. The AlN wide-band gap, 6.3 eV, which makes it transparent in the visible spectrum, allows it to be utilized as a protective coating in optics. Furthermore, the good thermal conductivity, thermal expansion coefficient close to that of silicon, and insulation characteristics make AlN interesting in microelectronics. Yet, the literature does not show promising use of AlN thin films alone for applications where wear and corrosion are of primary concern, despite being a hard and chemically stable material.

In equilibrium Ti, Al and N show insolubility in the AlN, TiN and TiAl phases, respectively, but they could be in solid solution in TiN and AlN when the production process is far from equilibrium conditions. In the Ti–Al–N system, the $Ti_{1-x}Al_xN$ with $x = 0.5$ has been developed as an alternative coating material for structural applications, where TiN has not demonstrated a good performance, particularly if the environmental atmosphere has a low humidity and/or the contact temperature is high enough to require high oxidation resistance of the component/tool surface, as in high-speed cutting. Incorporation of Al into TiN thin films improves the oxidation behaviour and the thermal stability of the coating. The cutting behaviour of (Ti, Al)N is not only superior to that of other conventional binary coatings but can also be used at significantly higher cutting speeds [12, 13]. In addition, the oxidation resistance of cutting tools coated with $Ti_{1-x}Al_xN$ thin films can also be improved [14]. Aside from the $Ti_{0.5}Al_{0.5}N$ thin films widely used in the industry of mechanical components and tools, other chemical compositions, lacking in popularity and characterized by Ti/Al and (Ti + Al)/N ratios different from unity, could exhibit good performances in hardness [15, 16] and wear/corrosion behaviour [17].

The aim of the present paper is to compile the master structural characteristics of binary and ternary thin films, with elemental contents different from the conventional ones, but produced using similar deposition approaches. The objective is to establish the fundamental aspects of the atomic structure, the preferred orientation and the morphology of 2D monolithic materials belonging to the Ti–Al–N system. The effect of the second and third element in structural order will be highlighted.

In the ternary diagram of Fig. 1 the chemical compositions of all the thin films studied are represented, including

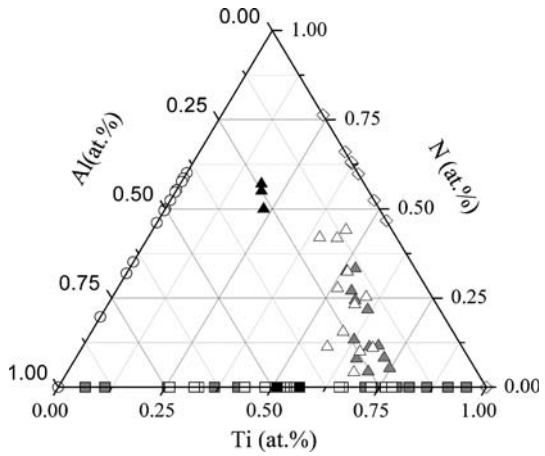

Fig. 1 Chemical composition of the thin films sputtered from γ-TiAl, composite and dual targets (respectively, black, grey and white symbols)

those of the Ti–Al, Ti–N and Al–N binary systems. The binary thin films will be discussed first, followed by the ternary ones, both categories presented with the goal in mind of using these thin films for industrial applications. The implications of the chemical composition/structure on hardness will be emphasized.

Binary systems

Ti–Al

References to sputter-deposited TiAl alloys date back to the early nineties [18, 19]. Since then, magnetron sputtering has been used to produce thin films of the Ti–Al system using different processing strategies, namely concerning the target(s) from which the films are sputtered. In fact, looking through the available literature it is possible to verify that TiAl thin films can be produced using composite targets (Ti target(s) with Al inserts or vice versa), dual targets (two or more pure metal targets), and γ-TiAl alloy targets. Whatever the chemical composition and the configuration of the target(s) used to produce the Ti–Al thin films, the as-deposited morphology is type T, quite dense (almost featureless), according to the Thornton model. Another common feature of these films is their nanometric grain size.

Using composite targets it is possible to cover the entire Ti–Al composition range by varying the number and size of the targets' inserts. Using dual targets it is also possible to cover a wide range of chemical compositions by adjusting either the Ti and Al targets' power supplies or current densities. Depending on the chemical composition, but also on the deposition strategy adopted, the as-deposited structure of the films could be indexed as α-Ti, Al or both (Fig. 2 and Table 1). This study also revealed that an amorphous phase

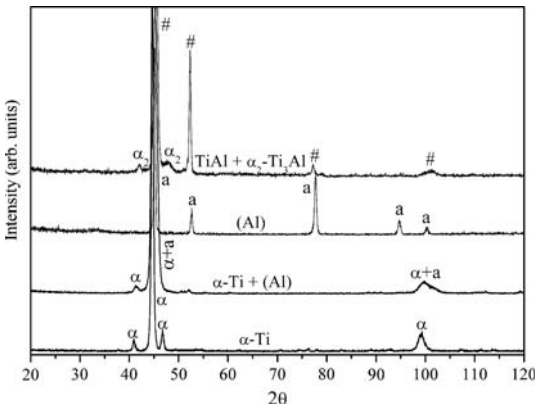

Fig. 2 Typical structure of as-deposited Ti–Al thin films deposited using composite, dual and γ-TiAl targets. α: α-Ti, a: Al, #: disordered TiAl, α_2: α_2-Ti_3Al

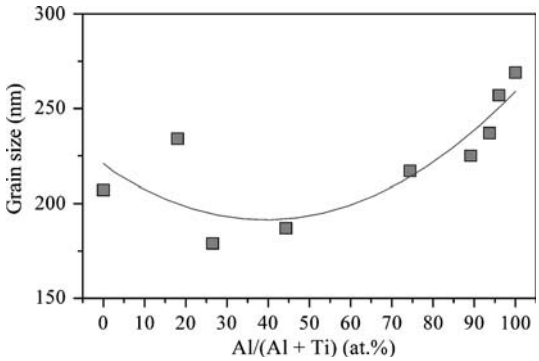

Fig. 3 Grain size as a function of aluminium content in Ti–Al thin films prepared using a composite target (From C. Coelho, MSc. Thesis. University of Coimbra, Portugal, 1999)

Table 1 Structure of as-deposited Ti–Al thin films as a function of the aluminium content

Composite target(s)			
Al (at.%)	0 ↔ 55	55 ↔ 65	65 ↔ 100
Structure	α-Ti(Al)	Amorphous	Al(Ti)
Dual targets			
Al (at.%)	22 ↔ 75		
Structure	α-Ti + Al		
γ-TiAl target			
Al (at.%)	44 ↔ 48		
Structure	Disordered TiAl + α_2-Ti_3Al		

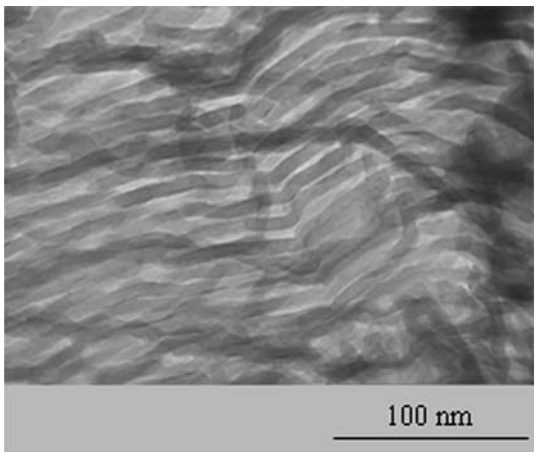

Fig. 4 TEM top view image of an as-deposited Ti–48Al thin film produced using two pure metal targets. Dark-grey layers correspond to Ti-rich phase and light-grey layers to Al-rich phase

is present in the range of the solute oversaturation (Table 1). In fact, according to Fig. 3, the solute in solution induces a decrease of the crystallite size independently of the solute's being Ti or Al [20]. It should be noted that when using a Ti target with Al inserts, the aluminium solubility is extremely extended (up to 50.5 at.%), while the use of two targets is responsible for a biphasic structure consisting of two solid solutions, one Ti-rich, (α-Ti), and the other Al-rich, (Al). In this case, the deposition procedure gives rise to a nanometric multilayer whose single-layer thickness (period) is a function of the time that the substrates are in front of each target during one rotation [21]. For the lowest aluminium content (27 at.%), the Al-rich single layers are extremely thin (<1 nm) and this element could diffuse into the Ti-rich layers during the deposition process. This result is sustained by the fact that the aluminium is the dominant diffusion specie in the Ti–Al system. The layered structure of an as-deposited Ti-48Al multilayer thin film with nanometric period is illustrated in the transmission electron microscopy (TEM) image of Fig. 4, where the Ti and Al layers could be identified. Also, due to the aluminium diffusion, the Ti layers are thicker than the Al ones.

Thin films with aluminium contents close to 44–48 at.% could be deposited from sputtering a γ-TiAl target with a similar chemical composition at a substrate temperature around 300–400 °C. In this case the X-ray diffraction pattern of this film is indexed as disordered TiAl plus α_2-Ti_3Al (Fig. 2), which is also not the equilibrium structure (γ-TiAl + α_2-Ti_3Al). For low substrate temperatures, the production of amorphous Ti–Al thin films is commonly referenced in the literature [19, 22, 23]. Some authors also mentioned the production of γ-TiAl as-deposited films, but always by heating the substrates [8, 19, 23]. The structures of the different Ti–Al thin films, sputtered from composite, dual or γ-TiAl targets, are summarised in Table 1. Whatever the deposition strategy used, the resulting atomic structures are not consistent with thermodynamic equilibrium. For near equiatomic chemical compositions and for the adopted deposition strategies, the γ-TiAl equilibrium phase, with or without small amounts of α_2-Ti_3Al, is achieved after an anisothermal heating (10 °C min^{-1}) up to 800 °C.

In the Ti–Al thin films, the aluminium content influences the hardness, whose values are always higher than the hardness of pure Ti thin films (6.8 GPa), which in turn are significantly harder than bulk titanium (1.5 GPa). The hardness of Al thin films (1.7 GPa) is also higher than that of bulk aluminium, as is usually observed by sputtering other elements/compounds [24]. In the case of the films prepared using composite targets, a solid solution hardening due to lattice distortions must occur. For the films sputtered from dual targets, the hardness increase could be attributed to the layered structure. In fact, nano-scale multilayers often show large hardness enhancement compared with monolithic coatings, depending this enlargement on the modulation period. The effect of Al was studied by evaluating the hardness of some Ti–Al thin films prepared using composite and dual targets (Fig. 5). For both targets' configuration, the hardness increases with the Al content up to the maximum observed, which was at a Ti/Al ratio close to 3. Increasing further the Al content leads to lower hardness values in agreement with the presence of the Al soft-phase in the films sputtered from dual targets. The thin films with near-equi-atomic chemical composition were heat treated at 600 °C for 1 h; a hardness increase was observed (9.5 GPa compared to 12.6 GPa) due to the formation of the ordered γ-TiAl phase. Once again, the thin films' hardness is higher than the corresponding bulk value (≈3–5 GPa).

Ti–N

Thin films from the Ti-N system comprise three distinct phase domains depending on the nitrogen content: α-Ti up to N/Ti = 0.2, Ti_2N for 0.2 < N/Ti < 0.6 and $Ti_{1-x}N_x$ for N/Ti ≥ 0.6. In the available literature, no references of intermediary amorphous stages along the sequence α-Ti(N) → Ti_2N → TiN were found.

Titanium nitride thin films deposited by PVD processes are stable over a wide chemical composition range but, like other nitrides of transition metals such as tungsten, their structure and properties are strongly dependent on their divergence from stoichiometry [25]. Cubic $Ti_{1-x}N_x$ is stable over a broad composition range ($0.6 \le x \le 1.2$) and appreciable vacancy concentrations (up to 50 at.%) [26]. Besides the chemical composition, also the thermal expansion coefficients mismatching between the coating and the substrate, which causes an important stress state in the coatings, can promote a shift in the lattice parameter. The highest hardness values of $Ti_{1-x}N_x$ thin films are found at nitrogen-to-titanium ratios of approximately 0.6, attaining values of 40 GPa [10]. The high hardness values are associated with high levels of intrinsic stress. For overstoichiometric coatings, hardness drops abruptly to values of 3.5 GPa for a nitrogen-to-titanium ratio of 1.2 [10]. Near-stoichiometric TiN thin films (20–30 GPa) are the ones most often used as wear resistant coatings for cutting tools. For the Ti_2N phase domain, the hardness values lie between 15 and 30 GPa [10].

In spite of the wide range of applications of TiN coatings, they present some disadvantages, foremost among which is their oxidation at relatively low temperatures, ~500 °C. Ternary thin films could be a solution to overcome this problem.

Al–N

Al–N thin films with nitrogen contents up to ≈60 at.% were deposited by reactive r.f. magnetron sputtering from a pure Al target. The f.c.c. aluminium phase was indexed from X-ray diffraction patterns for the films with low nitrogen contents (Fig. 6). The study of the chemical composition evolution with nitrogen content shows that it is possible to

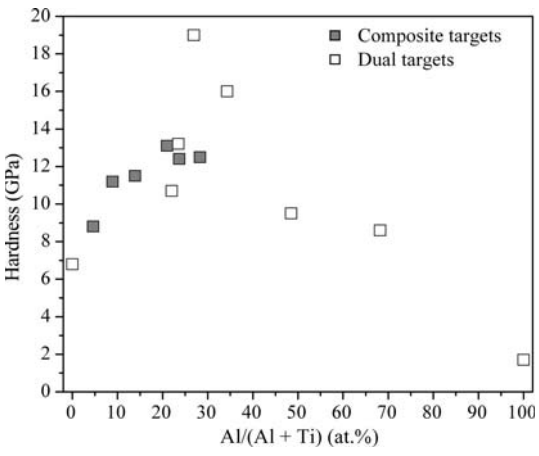

Fig. 5 Hardness as a function of aluminium content in Ti–Al thin films

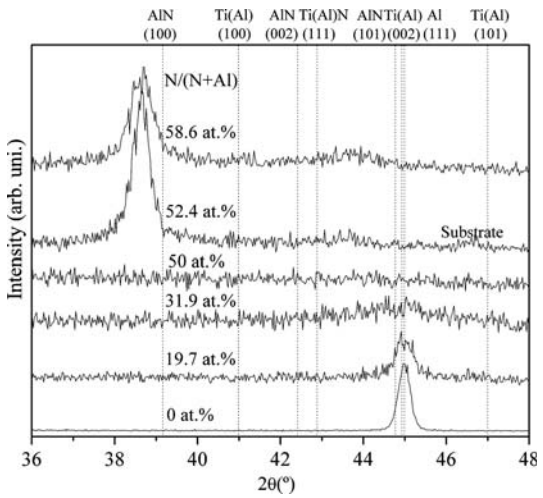

Fig. 6 X-ray diffraction patterns of Al–N thin films

incorporate by magnetron sputtering up to ≈32 at.% N in the f.c.c Al structure. However, the increase in nitrogen incorporation in the cubic structure leads to a progressive enlarging of the (111) diffraction peak with loss of intensity, corresponding to a high density of defects and a failure of crystallinity of the structure. The excess of nitrogen in grain boundaries could control the grain size growth during the deposition of the thin films, as in other metals where the excess of an interstitial element controls the crystallite size [27]. At intermediate nitrogen contents, the h.c.p. AlN phase with a preferential orientation along (100) appears, first with a well-defined peak and subsequent peak enlargement. The transformation of the interstitial solid solution to a new compound has an intermediate amorphous phase: Al(N) → amorphous → AlN. As compared to stoichiometric AlN, the excess of nitrogen measured in some of these films was attributed to the incorporation of the N atoms in the interstitial position of the h.c.p. AlN lattice, as indicated by the high *c/a* ratio resulting mainly from high *c* parameter values. This result may be due to implantation of nitrogen atoms at the film surface during film growth as proposed by Tominaga et al. [28]. The hardness of the h.c.p. AlN thin films ranges from 13 to 16 GPa.

Ternary system

Ti–Al–N thin films were deposited by reactive magnetron sputtering in different N_2/Ar atmospheres using the three target configurations already mentioned for the Ti–Al binary films: composite, dual and γ-TiAl targets (Fig. 1).

N on Ti ≫ Al

The first Ti–Al–N thin films deposited had nitrogen contents up to 42 at.% and were prepared by magnetron sputtering using composite and dual targets. The Ti content was always close to 2.5–3.5 times that of Al. In the Ti–Al system, as already indicated, the presence of Al in the Ti is possible up to high contents, with a decrease of *a* lattice parameter (Table 2). The difference observed in thin films deposited using composite versus dual targets results from the localisation of Al in the Ti lattice. For thin films deposited from composite targets, the Al is in substitution in the Ti lattice, but for those resulting from dual targets most of the Al content must be as a very thin interlayer not discernable by X-ray diffraction.

In Fig. 7 and 8, the influence of the nitrogen content on the structure of these Ti–Al–N thin films is shown. The h.c.p. Ti phase is indexed in X-ray diffraction patterns for thin films with low nitrogen contents. In the thin films resulting from composite targets, the preferential orientation is still (002) with the presence of N, indicating that nitrogen is in the Ti lattice. The angle of diffraction decreases as the deposition flow of N increases. In thin films deposited from dual targets up to 10 at.% nitrogen no change in preferential orientation is observed, but for high values of N (as 23.2 at.%) the (002) Ti peak is completely dominant. As the nitrogen content increases, the Ti (002)

Table 2 Lattice parameters (nm) of Ti–Al–N thin films

	Nitrogen content (at.%)			
	0	<5	<11	<25
Composite targets	a = 0.292	a = 0.294	a = 0.296	
	c = 0.474	c = 0.474	c = 0.474	
Dual targets	a = 0.295		a = 0.296	a = 0.296
	c = 0.474		c = 0.477	c = 0.479

Pure Ti: a = 0.2950; c = 0.4683

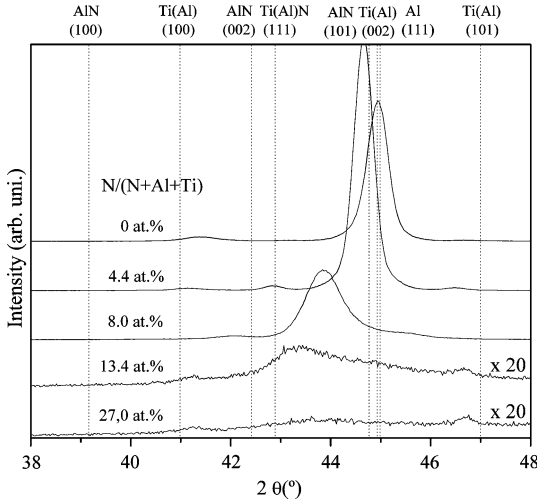

Fig. 7 X-ray diffraction patterns of Ti–Al–N thin films sputtered from composite targets as a function of nitrogen content

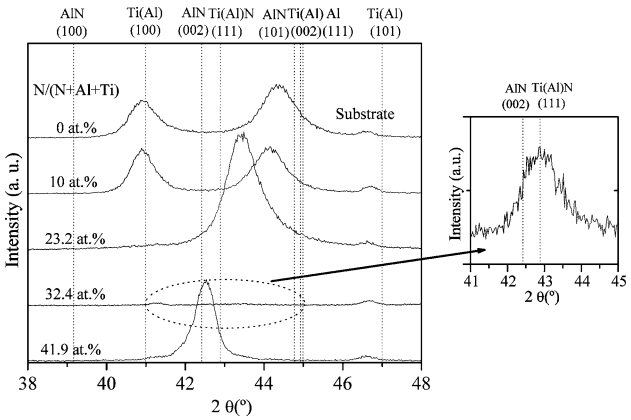

Fig. 8 X-ray diffraction patterns of Ti–Al–N thin films sputtered from dual targets as a function of nitrogen content

peak shifts to lower diffraction angles due to the incorporation of N in interstitial positions within the α-Ti crystalline lattice. By magnetron sputtering it was possible to incorporate nitrogen into the α-Ti lattice at up to 8 or 23 at.%, for composite or dual targets, respectively. In both cases, intermediate N contents favour the loss of crystallinity. For composite targets, the presence of nitrogen induces an increase of the lattice parameter *a* towards that of the Ti lattice without Al. This could be attributed to the presence of N in the network associated with a decline of Al atoms in substitution in the Ti lattice, which limits the grain size. In fact, for composite targets a significant decrease in the Ti crystallite size and loss of intensity of Ti peak diffraction is observed for N contents lower than in dual targets' sputtered thin films. In this case, the presence of N only contributes to an increase of the *c* lattice parameter. For high N contents, the thin films exhibit an f.c.c. TiN structure with (111) preferential orientation.

The influence of nitrogen on the hardness of Ti–Al–N (low content of Al) thin films, prepared using composite and dual targets, is illustrated in Fig. 9. For similar N contents the ternary films are always harder than the TiN and AlN ones. The hardness of the Ti–Al–N thin films deposited from composite targets increases gradually with the nitrogen content. Contrarily, the hardness of the thin films sputtered from dual targets is strongly related to their structure. In fact, a pronounced hardening is observed for the amorphous and Ti(Al)N thin films whose hardness values are somewhat higher than those measured for the films sputtered from a γ-TiAl target (26–30 GPa). This difference must be related to the thin films' chemical composition. The maximum hardness value (36 GPa) was measured for the film produced using dual targets enriched with at least 32.4 at.% N, which has an amorphous appearance and should correspond to a Ti(Al)N phase with extremely small nanocrystallites.

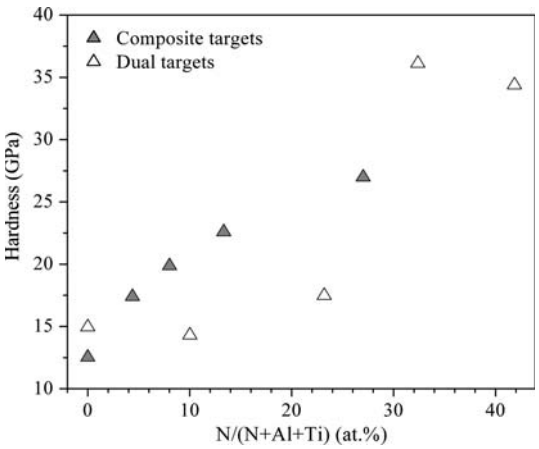

Fig. 9 Hardness as a function of nitrogen content in Ti–Al–N thin films

Barshilia et al. [29] showed that Al content influences the hardness of Ti–Al–N thin films, whose values decrease with increasing Al present in the TiAl target from which the films were sputtered.

N on Al ≫ Ti

As already observed for high Ti contents, the formation of nitrides is always preceded by a loss of crystallinity at intermediate N contents. According to Sanchette et al. [30], before amorphisation, thin films with 11 at.% Ti are single phase Al up to 10 at.% N, with smaller grain size as the nitrogen composition increases. Beyond a critical nitrogen fraction in the reactive gas mixture, a fine AlN precipitation is detected.

Al on $Ti_{1-x}Al_xN$

The most common thin films of this system, those that have attracted much attention in the recent past due their high speed cutting ability, have N contents close to 50 at.%. A large number of studies on this type of coating are available in scientific publications, particularly concerning the influence of Al content in phase constitution, preferential orientation and lattice parameters (Fig. 10 with included references). Some studies highlight the role of Al content in the phase evolution before and after applications [45]. The limit of Al content in substitution in titanium determines the occurrence of a high density of defects and a decrease of crystallite size of Ti(Al)N up to $x = 0.5$ [44]. For higher Al contents and before forming AlN, an amorphous phase is also present in a narrow composition range (50–60 at.%) [44]. According to Hultman [26], AlN is found as nanometric grains in the boundaries of Ti(Al)N grains. For the highest Al contents, a new h.c.p. AlN phase occurs and no peaks of TiN are observed by X-ray diffraction. The influence of Al content in mechanical properties such as hardness and Young's modulus as determined by some authors is compiled in Table 3.

N on $Ti_{1-x}Al_xN$ ($x = 0.5$)

Few studies have examined the influence of N on $Ti_{0.5}Al_{0.5}N$ thin films. Recently Singh et al. [17] studied the wear behaviour of $Ti_{1-x}Al_xN$ thin films sputtered from a composite target with equal Ti and Al areas under different nitrogen flows, but it was not quantified. Another study on the influence of nitrogen in the atomic structure variation results from sputtering a γ-TiAl target at various N_2/Ar ratios. The Al/Ti ratio in the thin films is slightly higher than 1. The nitrogen content varies from 50–60 at.%, respectively, for 1/3, 1/2 and 1 N_2/Ar ratios (see Fig. 1). The respective X-ray diffraction patterns are presented in Fig. 11. For these chemical

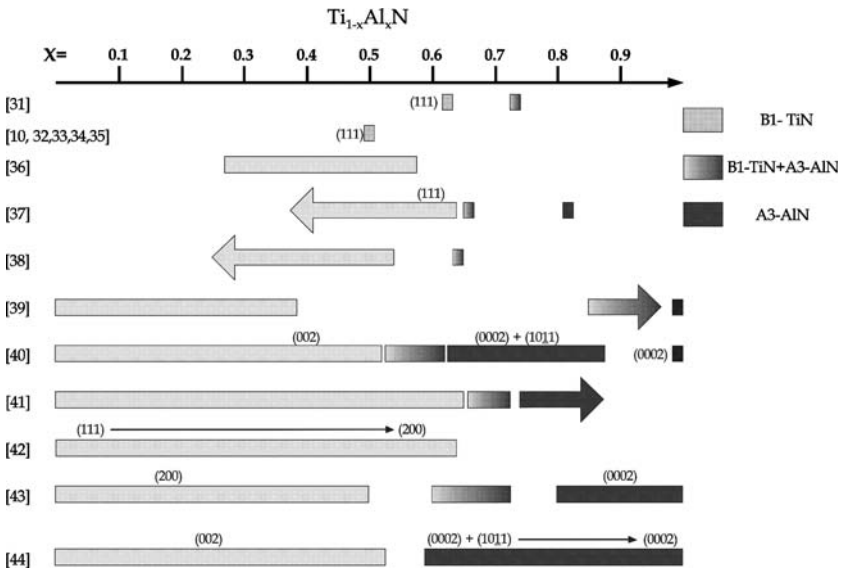

Fig. 10 Structure of $Ti_{1-x}Al_xN$ thin films function of the Al content

Table 3 Crystallite size, hardness and Young's modulus of $Ti_{1-x}Al_xN$ thin films

X ($Ti_{1-x}Al_xN$)	Crystallite size (nm)	Hardness (GPa)	Young modulus (GPa)	Authors
0.5	–	22–23	–	W-D Münz [12]
~0.5	105 → 35	10 → 42	–	G Håkansson et al. [33]
	↑ V_S	↑ V_S		
0.5	–	22–24	–	O Knotek et al. [46]
0.5	–	~36	–	B-Y Shew et al. [47]
$X \leq 0.46$	–	20–23	–	C Jarms et al. [39]
$X \geq 0.69$	–	12	–	
$0 \leq X \leq 0.60$	–	19 → 32	–	T Suzuki et al. [41]
$X \geq 0.69$	–	28 → 12	–	
$X \leq 0.52$	<30	35	–	P Panjan et al. [38]
0.64	30–60	17	–	
$X \leq 0.5$	–	26 → 40	360 → 650	M Zhou et al. [43]
$0.6 \leq X \leq 0.7$	–	33 → 22	500 → 420	
0.59	–	27	~400	J Musil and Hrubý [40]
↑ N	–	33		
	70 → 10	47		
	100 °C → 400 °C	T_d = 200 °C		
$X \leq 0.54$	–	16–34 (scattered results)	–	SK Wu et al. [42]
0.5	10	36 → 40	~450	KN Andersen et al. [34]
		↑ V_S 80 → 130		

V_S—substrate bias

compositions, the films always exhibit a B1-NaCl type structure indexed as TiN, but as expected with the (111) and (200) peaks shifted to higher 2θ values. This shift is associated, as already discussed, with the shrinkage of the lattice parameter resultant from the substitution of Ti atoms in the TiN lattice by Al atoms with a smaller atomic radius (0.143 nm against 0.147 nm). However, the increase of nitrogen in the $Ti_{1-x}Al_xN$ structure decreases the shift to the right of the peaks due to the substitutional aluminium, as for Ti/Al > 2.5 with low percentages of N. The degree of nitrogen overstoichiometry in TiAlN increases the lattice parameter from 0.420 to 0.421 nm (values calculated by the Bradley-Jay method [48]). In the range of nitrogen content studied, the crystallite size is similar and no loss of crystallinity was observed. The highest hardness value is measured for the lowest N content (50 at.%)—35 GPa. The hardness decreases up to 30 GPa as the nitrogen in the thin film increases, which suggests the presence of h.c.p. AlN which is not yet

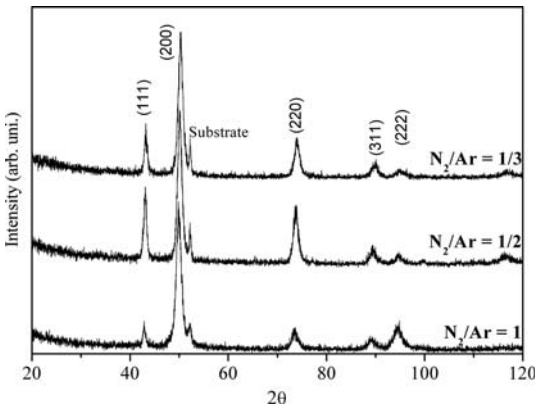

Fig. 11 X-ray diffraction patterns of Ti–Al–N thin films sputtered from a γ-TiAl target under various N_2/Ar atmospheres

distinguishable in the X-ray diffraction pattern. Many authors associate the presence of h.c.p. AlN to the falling of the $Ti_{1-x}Al_xN$ hardness.

For the selected conditions in the present study, with the introduction of nitrogen into Ti, Al and Ti–Al the thin films' cross-section turns out to be less dense and the morphology becomes compact columnar (Thornton type I) as exemplified in Fig. 12. Dense columnar morphology is

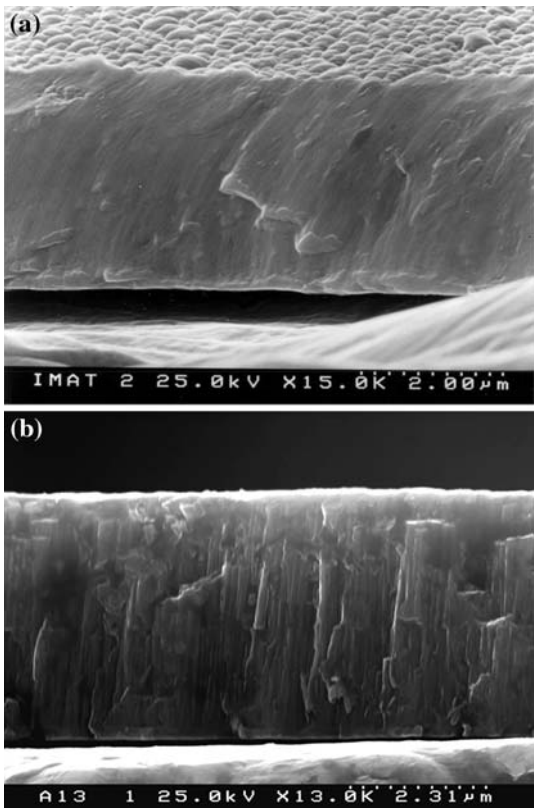

Fig. 12 SEM cross-section image of as-deposited (**a**) Ti–Al and (**b**) Ti–Al–N thin films

the most reported in the literature for $Ti_{1-x}Al_xN$ coatings [32, 33, 38, 39, 41, 49].

Summary

Thin films based on elements of the Ti–Al–N system were deposited by magnetron sputtering using essentially composite and dual targets. Ti–N, Al–N and especially thin films of the Ti–Al system were also investigated. Nearly one hundred different chemical compositions in the Ti–Al–N ternary system were studied. The targets' configuration and chemical composition determine the atomic structure and the degree of crystallinity of the thin films and consequently influence their hardness.

The aluminium in solid solution in the Ti–Al thin films prepared using composite targets induces a significant decrease in the a lattice parameter and crystallite size before becoming Ti in solid solution in an Al matrix. The hardness increases with the solute Al content in solid solution up to a maximum which corresponds to the matrix modification. On the other hand, dual targets lead to a multilayer thin film of Ti and Al, with the Ti lattice parameter unchangeable. The hardness results from the Ti and Al layers. The introduction of nitrogen into thin films with low Al contents favours the loss of crystallinity. In fact, X-ray diffraction patterns characteristic of an amorphous phase are observed in thin films with 10 and 32 at.% N for composite and dual targets, respectively. The intermediary amorphisation is related to the decrease of aluminium in solid solution ($a \uparrow$). For high Al contents, Ti is in solid solution in an Al matrix and 10 at.% N is enough to reduce significantly the grain size. This behaviour is similar to the Al–N binary system. In $Ti_{1-x}Al_xN$ thin films, Ti and Al similar contents do not induce loss of crystallinity, not even for an overstoichiometry in N that only contributes to decrease the hardness as in the Ti–N binary system. For $Ti_{1-x}Al_xN$ thin films, the Al in solid solution in TiN induces a significant decrease in the crystallite size before being AlN with Ti in the matrix. In this case, $x = 0.55$ results in amorphous thin films.

In general, a loss of crystallinity is observed in the transition from a saturated solid solution to a new compound (intermediary amorphous stage).

Acknowledgments This work was supported by Fundação para a Ciência e Tecnologia, BPD/6771/2001, and FEDER.

References

1. Kim HC, Theodore ND, Gadre KS, Mayer JW, Alford TL (2004) Thin Solid Films 460:17

2. Wendler B, Danielewski M, Przybylski K, Rylski A, Kacmarek L, Jachowicz M (2006) J Mater Proc Technol 175:427
3. Escudero ML, Muñoz-Morris MA, Garcia-Alonso MC, Fernández-Escalante E (2004) Intermetallics 12:253
4. Kim Y-W (1994) JOM 46:30
5. Vieira MT, Trindade B, Ramos AS, Fernandes JV, Vieira MF (2000) Surf Coat Technol 131:162
6. Vieira MT, Trindade B, Ramos AS, Fernandes JV, Vieira MF (2002) Mater Sci Eng A 329:146
7. Vieira MT, Roque S, Ramos AS (2000) Adhes Aspects Thin Films 1:171
8. Lii D-F, Huang J-L, Lin M-H (1998) Surf Coat Technol 99:197
9. Ramos AS, Vieira MT, Duarte LI, Vieira MF, Viana F, Calinas R (2006) Intermetallics 14:1157
10. Sundgren J-E, Hentzell TG (1986) J Vac Sci Technol A 4:2259
11. Oliveira JC, Cavaleiro A, Vieira MT (1999) In: Proceedings of the 13th conference on surface modification technologies, 1999
12. Münz W-D (1986) J Vac Sci Technol A 4:2717
13. Khrais SK, Lin YJ (2007) Wear 262:64
14. Huang J-L, Shew BY (1999) J Am Ceram Soc 82:696
15. Oliveira JC, Manaia A, Dias JP, Cavaleiro A, Teer D, Taylor S (2006) Surf Coat Technol 200:6583
16. Kim GS, Lee SY, Hahn JH (2005) Surf Coat Technol 193:213
17. Singh K, Limaye PK, Soni NL, Grover AK, Agrawal RG, Suri AK (2005) Wear 258:1813
18. Yan Q, Yoshioka H, Habazaki H, Kawashima A, Asami K, Hashimoto K (1990) J Non-Cryst Solids 125:25
19. Silvain JF, Barbier JE, Lepetitcorps Y, Alnot M, Ehrhardt JJ (1993) Surf Coat Technol 61:245
20. Sanchette F, Billard A, Frantz C (1998) Surf Coat Technol 98:1162
21. Gachon J-C, Rogachev AS, Grigoryan HE, Illarionova EV, Kuntz J-J, Kovalev DYu, Nosyrev AN, Sachkova NV, Tsygankov PA (2005) Acta Mater 53:1225
22. Banerjee R, Swaminathan S, Wheeler R, Fraser HL (2000) Phil Magazine A 80:1715
23. Padmaprabu C, Kuppusami P, Singh A, Mohandas E, Raghunthan VS (2001) Scripta Mater 44:1837
24. Rickerby DS, Burnett PJ (1998) Thin Solid Films 157:195
25. Castanho JM, Vieira MT (1998) Surf Coat Technol 102:50
26. Hultman L (2000) Vacuum 57:1
27. Pierson JF, Wiederkehr D, Billard A (2005) Thin Solid Films 478:196
28. Tominaga K, Imai H, Shirai M (1991) Jpn J Appl Phys 30:2574
29. Barshilia HC, Prakash MS, Jain A, Rajam KS (2005) Vacuum 77:169
30. Sanchette F, Loi TH, Billard A, Frantz C (1995) Surf Coat Technol 74–75:903
31. Witthaut M, Cremer R, Von Richthofen A, Neuschütz D (1998) Fresenius J Anal Chem 361:639
32. Jehn HA, Hofmann S, Münz W-D (1987) Thin Solid Films 153:45
33. Håkansson G, Sundgren J-E, McIntyre D, Greene JE, Münz W-D (1987) Thin Solid Films 153:55
34. Andersen KN, Bienk EJ, Schweitz KO, Reitz H, Chevallier J, Kringhøj P, Bøttiger J (2000) Surf Coat Technol 123:219
35. Prengel HG, Santhanam AT, Penich RM, Jindal PC, Wendt KH (1997) Surf Coat Technol 94–95:597
36. Huang CT, Duh J-G (1996) Surf Coat Technol 81:164
37. Vaz F, Rebouta L, Andritschky M, Silva MF, Soares JC (1997) J European Ceram Soc 17:1971
38. Panjan P, Navinšek D, Čekada M, Zalar A (1999) Vacuum 53:127
39. Jarms C, Stock H-R, Mayr P (1998) Surf Coat Technol 108:206
40. Musil J, Hrubý H (2000) Thin Solid Films 365:104
41. Suzuki T, Huang D, Ikuhara Y (1998) Surf Coat Technol 107:41
42. Wu SK, Lin HC, Liu PL (2000) Surf Coat Technol 124:97
43. Zhou M, Makino Y, Nose M, Nogi K (1999) Thin Solid Films 339:203
44. Wahlström U, Hultman L, Sundgren J-E, Adibi F, Petrov I, Greene JE (1993) Thin Solid Films 235:62
45. Karimi A, Vasco Th, Santana A (2005) In: Basu SN, Krzanowski JE, Patscheider J, Gogotsi Y (eds) Surface engineering 2004—fundamentals and applications, Mater Res Soc Symp Proc 843, Warrendale, PA, T3.38
46. Knotek O, Münz W-D, Leyendecker TJ (1987) J Vac Sci Technol A 5:2173
47. Shew B-Y, Huang J-L, Lii D-F (1997) Thin Solid Films 293:212
48. Suryanarayana C, Norton MG (1998) X-ray diffraction: a pratical approach. Plenum Press
49. Cunha L, Andritschky M, Rebouta L, Silva R (1998) Thin Solid Films 317:351